JMEPEG (2004) 13:185-194
DOI: 10.1361/10599490418460

1059-9495/$19.00

Stripping Methods Studies for HVOF WC-10Co-4Cr Coating Removal

Richard Menini, Nihad Ben Salah, and Rachid Nciri

(Submitted 21 November 2003; in revised form 12 January 2004)

The use of high-velocity oxyfuel (HVOF) cermet coatings is considered to be a valuable and innovative alternative technology to replace Cr(VI) electroplating. Among others, a WC-10Co-4Cr coating is one of the best choices for landing gear components due to its excellent tribology and corrosion properties. The stripping process of such a cermet coating was studied due to its importance for the repair and overhaul of landing gear components. Stripping solutions fulfill the following criteria: keep substrate integrity; exhibit a high strip rate (SR); lead to uniform dissolution; show no galvanic corrosion; and be environmentally friendly. Three different high-strength steel substrates (4340, 300M, and Aermet100) were studied. Five different stripping solutions were selected for the electrochemical study. Only three met the targeted criteria: the meta-nitrobenzane sulfonate-sodium cyanide solution; the Rochelle salt; and a commercial nickel stripper. It was found that the process must be electrolytic, and that ultrasonic agitation is needed to enhance the overall mass transport and removal of WC particles and metallic matrix residues. When choosing the most efficient solution and conditions, the SR was found to be as high as 162 μm h^{-1}, which is a very acceptable SR for productivity sake.

Keywords: cermet, chemical stripping, corrosion, electrolytic stripping, high-strength steel, HVOF coating, maintenance, overhaul, repair

1. Introduction

In several industrial sectors, hard chrome plating is a major process that has been used in commercial production for over 50 years. In some industrial processes, the use of chromium in its hexavalent state, Cr(VI), is necessary to produce the hard chromium plating. However, for environmental reasons,[1] the industries that are using Cr(VI) have been urged to comply with its permissible exposure limit (0.1 mg/m^3) value limitation[2] for the next few years, which could result in high cost investments to modify current processes. The aircraft industry currently uses hard chromium plating for landing gear and/or aircraft actuator components, but it is developing alternative processes to replace the use of Cr(VI).

The use of high-velocity oxyfuel (HVOF) cermet coatings has been considered as a valuable and innovative alternative technology to replace Cr(VI).[3,4] The WC-10Co-4Cr coating has been shown to be an adequate choice for landing gear components due to its excellent tribological and corrosion properties.[5] Although this coating is the most promising, its productivity is still being studied in terms of its grinding, stripping, and inspecting capabilities.

The stripping process is of great importance for industries involved in the repair and overhaul of aircraft components.[6,7] This article describes the activities undertaken to determine an appropriate method for WC-10Co-4Cr HVOF coating removal for repair and overhaul of components in the aircraft industry. Joint laboratory and near-production testing that linked elec-

Richard Menini, Industrial Materials Institute, NRC-CNRC, 75 de Mortagne Boulevard, Boucherville, PQ, J4B 6Y4 Canada; and **Nihad Ben Salah** and **Rachid Nciri,** Héroux-Devtek, Landing Gear Division (Engineering), 1010 de Serigny, Suite 350, Longueuil, PQ, J4K 5G7 Canada. Contact e-mail: richard.menini@cnrc-nrc.gc.ca.

Nomenclature

η	overvoltage ($E - E_{corr}$), V
ρ	density, kg m^{-3}
CPR	dissolution rate (100% efficiency), mpy (mils per year)
E	potential, $V_{/SCE}$
E_A	anodic potential, $V_{/SCE}$
E_C	cathodic potential, $V_{/SCE}$
E_{corr}	corrosion potential, $V_{/SCE}$
F	Faraday constant, 96484.6 C $equiv^{-1}$
FR	faradic rate, %
h_f	final thickness, μm
h_i	initial thickness, μm
i	current, A
j	current density, A cm^{-2}
j_o	corrosion current density, μA cm^{-2}
m	mass, kg
M	molar mass, kg
n	number of electron involved, -
Q_A	applied charge, C
Q_{Co}, Q_{Cr}	charge, C
Q_h	theoretical charge for ($h_i - h_f$) thickness, C
R_{cell}	solution resistance, Ω
R_{circ}	circuit resistance, Ω
RT	room temperature 25 °C
SCE	standard calomel electrode, -
SR	strip rate, μm h^{-1}
t, t_y	time, 1 year, s
U	electrolytical potential, V
v	scan rate (cyclic voltammetry), mV s^{-1}

Table 1 High Strength Steel Alloy Specifications

Substrates	AMS	Ultimate Tensile Strength, ksi	Finish for Bare Substrate Studies, μm
4340	6414	260-280	0.425
300M	6257	280-300	0.559
Aermet100	6532	280-300	0.159

trochemical data to simulation was performed to implement the stripping process at the production level.

The objectives of this study were to identify the best stripping solutions and methods according to the following criteria:

(i) The strippers should not etch or strip the material substrate.
(ii) The strip rate (SR) should be as high as possible.
(iii) The stripper should remove the coating as uniformly as possible, and it should not cause galvanic corrosion between the coating and the substrate.
(iv) The chemicals should not be harmful or hazardous to the environment.

Overall, three different high-strength steels substrates (4340, 300M, and Aermet100), which are commonly used in the landing gear industry, were coated with WC-10Co-4Cr, and five different stripping solutions were studied by electrochemical means to meet the above-mentioned criteria. Chemical and electrolytic methods were tested, as was the enhancement of the stripping process by ultrasonic agitation of the solutions.

2. Experimental

2.1 Sample Preparation

The three high-strength steel substrates studied are described in Table 1. Plate substrates (2.54 × 10.16 × 0.64 cm) were polished to assess the chemical and electrochemical behavior of the bare materials. All the specimens, bare or coated, were stored in desiccators when they were not in use. Coated tubular samples (5.08 OD × 4.06 ID × 10.16 length × 0.64 cm thickness) were also assessed for electrolytic stripping. Tube and plate specimens were machined before heat treatment, then were ground and shot peened.

The three different substrates were coated with WC-10Co-4Cr by the HVOF technique. The deposition conditions used were optimized in past studies.[5] Coatings were applied using a DJ-2600 gun with hydrogen and a SM-5847 powder. Prior to coating, substrate surfaces were carefully cleaned and grit blasted using 54-grit alumina at 60 pounds per square inch (psi), with a distance of 10.16-15.24 cm at an angle of 15° to 45°. The coating was built up to a thickness in the range of 100-200 μm. The final polishing step was performed using a 3 μm diamond paste.

2.2 Stripping Solutions

Two different groups of stripping solutions, S1(x) and S2(x) (Table 2), were chosen according to their abilities to strip nickel and chromium [S1(x)][8] and WC-xCo coatings [S2(x)].[9]

Table 2 List of Used Stripping Solutions and Their Specific Operating Conditions

Group	Chemical Composition	Operating Condition
S1	(1) NaOH (52 g/l) and Na carbonate (68 g/l) (Cr strip)	Electrolytic (a) 4 to 6 V, RT, pH, 14-15
	(2) NaOH (75 g/l) (Cr strip)	Electrolytic (a) 6 V, RT, pH, 14-15
	(3) Meta-nitrobenzane sulfonate (60 g/l), NaOH and Na cyanide (90 g/l) (Ni strip)	Chemical (a), 50 °C, pH, 11-12
S2	(1) Na carbonate and Na tartarate (Rochelle salts)	Electrolytic (b) 4 to 6 V, 65 °C, pH, 11-12
	(2) Commercial Nickel stripper	Chemical (b), 60 °C, pH, 9.5

(a) As per MIL-STD-871
(b) Usual conditions of operation

2.3 Electrochemical Measurements

The electrochemical experiments were conducted in aerated and magnetically stirred stripping solutions. A modified flat electrochemical cell (EG&G, Princeton Applied Research) was used with a platinum grid auxiliary electrode and a saturated calomel reference electrode (SCE). A specially designed glass coil was welded inside the cell to allow water circulation at a given temperature for thermostating purposes, and a condenser was added at the top of the cell. To avoid potential changes due to temperature, it must be pointed out that the reference electrode needed to be placed outside the main cell by means of a glass bridge filled with the stripping solution. All potentials quoted in the present article are in reference to the SCE. The electrochemical measurements were taken with a potentiostat (model 263A, Princeton Applied Research) that was controlled by a computer. The exposed surface area of the sample was 1 cm^2, and a special Teflon gasket was used for sealing and to avoid rim corrosion. At the end of each experiment, the sample was cleaned with acetone and water. The current density measurements on the cermet coatings were corrected by a 23% factor, since this value corresponds to the metallic fraction of the exposed surface area.[10]

Prior to making the Tafel plot recordings, corrosion potentials were determined after a 24 h period of stabilization. Thereafter, the potential was swept within a window of ±100 mV with respect to the stabilization potential at a scan rate of 0.05 mV s^{-1}. The corrosion current density values were calculated from the polarization curves (Tafel plots).[11] As far as cyclic voltammetry recordings were concerned, the samples were conditioned for 5 min at a potential ≈300 mV more cathodic than the corrosion potential, and subsequently the potential was scanned at 5 mV s^{-1} in the anodic direction to determine the anodic activity of the different studied materials and their ability to passivate. Following that scan, a cathodic sweep back to the initial potential was recorded to determine whether a stable oxide film covered the sample.

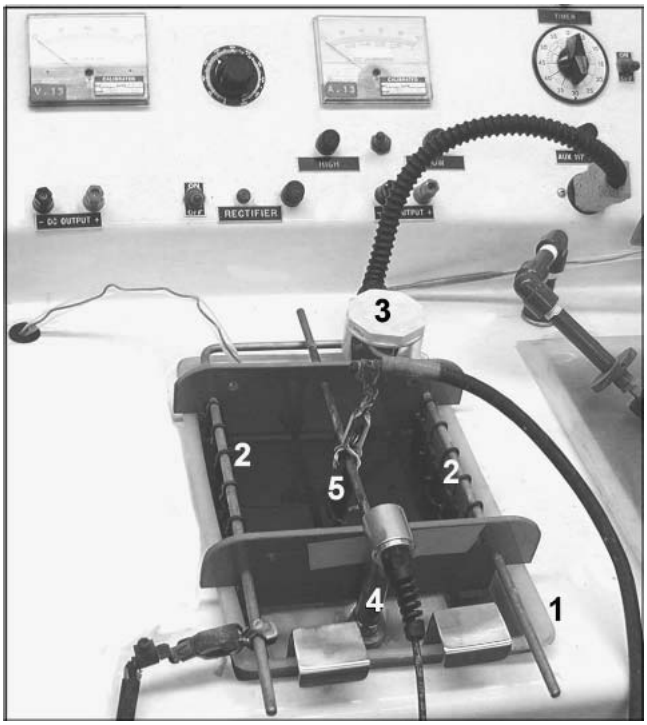

Fig. 1 Stripping mini-cell. **(1)** 10 L tank; **(2)** carbon steel cathodes; **(3)** heater; **(4)** ultrasonic transducer; and **(5)** coated specimen

2.4 Stripping Simulation Under Industrial Conditions

The five solutions were tested in a plating/stripping mini-cell to establish the industrial operational parameters. The tests were performed on the plate and on tubular specimens at three different potentials: 4, 6, and 7 V. Only conditions that permitted the entire removal of the coating in less than 24 h were retained. The electrochemical stripping process uses an anode in a 10 liter electrolytic tank containing cathodes (carbon steel) and the anode (the part to be stripped) immersed in the stripping solution (Fig. 1). To avoid the polarization of the fixtures (the cathode), the cathodic surface was made twice the size of the anodic surface. In addition, the cathode was not a one-piece fixture but was composed of different individual pieces to improve the current distribution. To improve the conduction of the current and to preclude the burning of the piece, the sample to be stripped was fastened to a steel bus bar with screws. An ultrasonic transducer (600 W and 40 kHz) was used to promote the stripping process. After every run, the thickness of the coating and the weight of the specimens were measured, and the surface appearance of the entire sample was inspected. Specimens were weighed on an analytical precision balance to 0.01 mg. For accurate measurements of the coating thickness (to a precision of 2.03 μm or 0.08 mils), a non-destructive device based on the eddy current principle was used. The average coating thickness loss was evaluated by taking 10 thickness readings in different locations. Each specimen was checked every 5 min until the coating had been completely removed. The specimen then was rinsed with hot tap water (49-60 °C) and with distilled water, and finally was blown dry with compressed air. In addition to coating thickness evaluation, a copper sulfate test was performed to ensure that the WC-10Co-4Cr coating was entirely removed (the solution turns red when in contact with steel substrates).

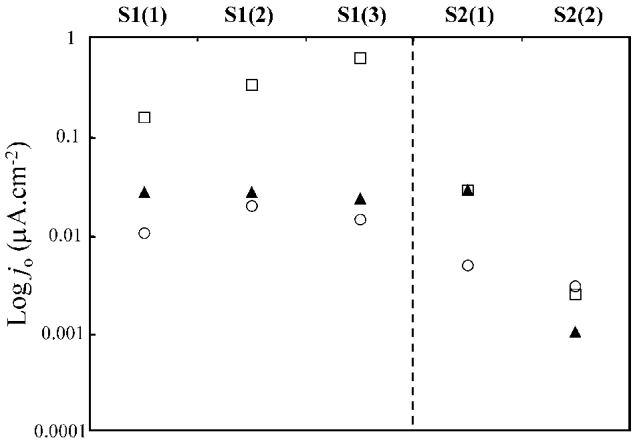

Fig. 2 Corrosion current densities vs S1 and S2 groups of strippers: ▲, 4340; □, 300M; and ○, Aermet100 bare substrates

3. Results and Discussion

3.1 Stripping Solutions Influence on Bare Steel Specimens

3.1.1 Corrosion Rates. To assess the behavior of the three substrates in the presence of the five stripping solutions, electrochemical studies were performed to extract the corrosion current densities from the Tafel plots [$\eta = f(\log j)$]. The corrosion current densities for S1 and S2 groups are displayed in Fig. 2.

Equation 1 was used to evaluate the corrosion penetration rate (CPR) in mils per year (mpy) of the substrate in a given solution. The units of the different variables or constants of Eq 1 are: A cm^{-2} for j_o, g cm^{-3} for ρ, s for t_y, g for M, and C for F. The calculation was performed assuming that only iron dissolution occurred, and that both the density and molecular weight were those of iron.

$$\mathrm{CPR} = \frac{1}{2.54 \times 10^{-3}} \times \frac{j_o M_{Fe} t_y}{n_{Fe} F \rho_{Fe}} \qquad \text{(Eq 1)}$$

For both the S1 and S2 groups, the maximum j_o value found, was 0.62 μA cm^{-2} for the 300M alloy in S1(3). This value corresponds to a CPR of 0.28 mpy, thus corresponding to a dissolution rate that is largely acceptable, since, in the case of a common stripping procedure, the solution could be in contact with the substrate for a maximum of 24 h. Moreover, optical microscope observations at high magnification (×800) showed no attack at the surface of the substrates after a 24 h immersion time. As shown in Fig. 2 for the S1 group of strippers (left-hand side), a hierarchy (from less resistant substrate to the most resistant one) can be established as follow:

300M < 4340 < Aermet100

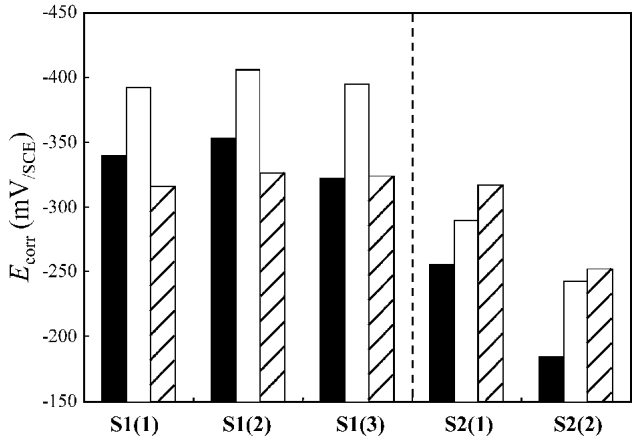

Fig. 3 Corrosion potentials vs S1 and S2 groups of strippers. Black bars, 4340 bare substrate; white bars, 300M bare substrate; and textured bars, Aermet100 bare substrate

For the S2 group (Fig. 2 on the right-hand side), no real hierarchy can be drawn since the three substrates are relatively inert to the two stripping solutions. The maximum CPR recorded was 0.0127 mpy (j_o = 27.5 nA cm^{-2}) for the 300M and the 4340 specimens in S2(1), while the minimum CPR was found at 4.5 × 10^{-4} mpy (j_o = 1 nA cm^{-2}) for the 4340 specimen immersed in S2(2).

3.1.2 Corrosion Potentials. The different values for the corrosion potentials are shown in Fig. 3 for the S1 and the S2 groups. Substrate corrosion resistance decreases with decreasing E_{corr} values (i.e., more cathodic values). Comparing the S1 and S2 groups, one can see that the S2 solutions were less corrosive than the S1 solutions, which confirms the conclusions drawn from the corrosion current density study. The hierarchy for the S1 group was the same as the one found for the corrosion current densities. The solutions of the S1 and the S2 groups did not etch or strip the three different substrates used in this study and, thus, did not meet criteria (i) in the Introduction. The Aermet100 was the most resistant alloy regarding all the tested solutions.

3.1.3 Passivation Ability. When it comes to choosing a proper stripping solution and conditions, it is important to avoid situations in which the coating passivates. To determine the abilities of the materials to passivate (i.e., to form a stable oxide layer), three different cyclic voltammetry studies were performed with the S1 and the S2 solutions, and the corresponding plots are shown in Fig. 4 and 5, respectively. The 4340 and 300M behaviors in the S1 solutions (Fig. 4a,b) show that these two materials exhibit a passivation behavior around 0.3 V in the S1(1) solution. This behavior is more difficult to detect for S1(2) and S1(3). However, some kind of protective films were probably formed since almost no cathodic activity is detected during the reverse scans. On the 300M specimen (Fig. 4b), one of the oxide or hydroxide films is not totally stable, and part of it is reduced around 0.4 V for the S1(1) and S1(2) solutions. The same observations can be made for the Aermet100 in the S1(1) stripping solution (Fig. 4c), where in this case three real passivation and transpassivation steps were clearly observed. These are probably due to the high percentage of oxidation of the alloying elements present in the

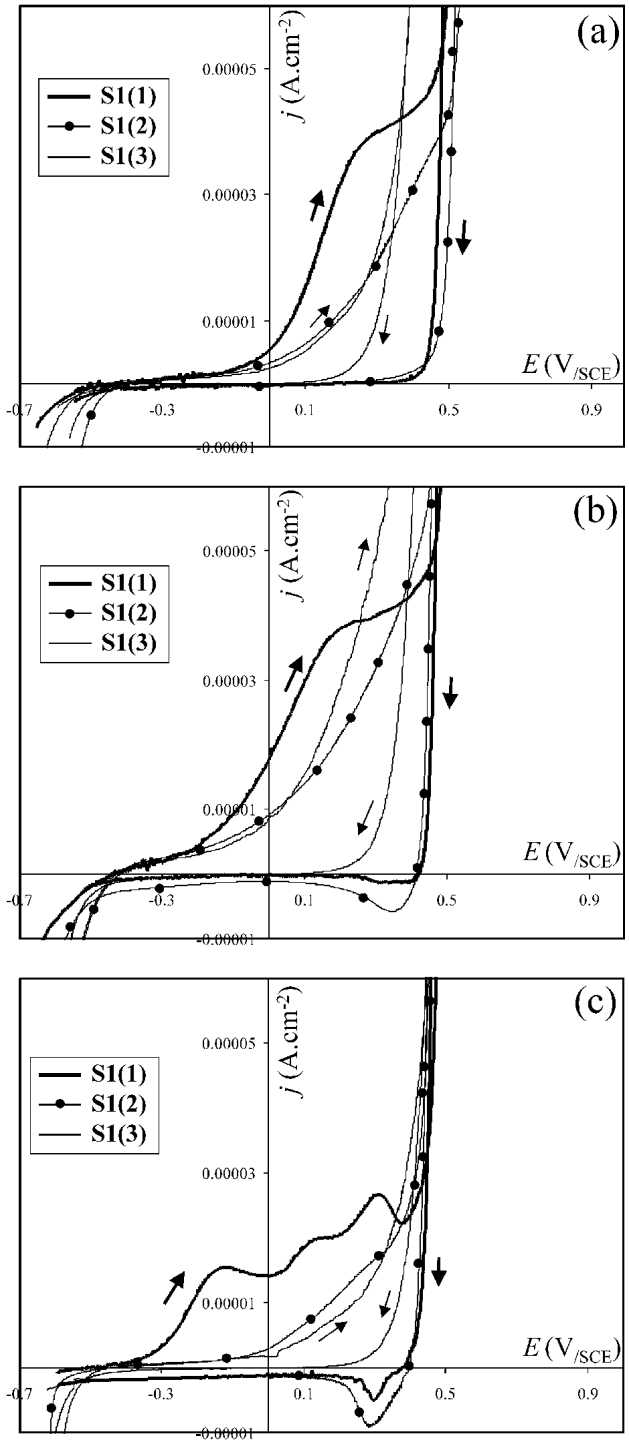

Fig. 4 Cyclic voltammetry plots for the S1 group. **(a)** 4340 bare substrate; **(b)** 300M bare substrate; and **(c)** Aermet100 bare substrate (v = 5 mV s^{-1})

Aermet100 (11.5% and 13.5%, respectively, for Ni and Co) compared with the lower alloy content for the 300M and the 4340. For the S1(3) solution, no peaks were visible and no anodic activity was observed for the three steel substrates on the back scans (Fig. 4a-c), which means that a thin layer of a

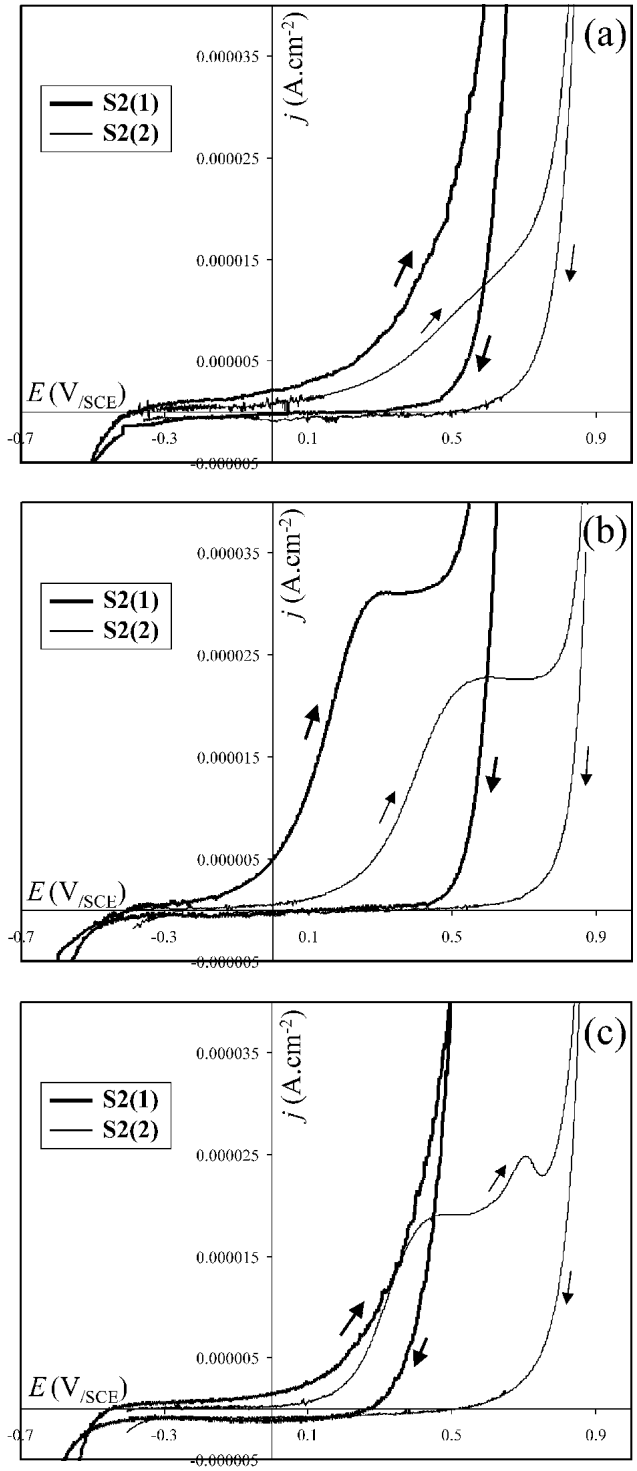

Fig. 5 Cyclic voltammetry plots for the S2 group. **(a)** 4340 bare substrate; **(b)** 300M bare substrate; and **(c)** Aermet100 bare substrate (v = 5 mV s^{-1})

stable oxide was formed in these conditions. Concerning the S2(1) solution no passivation or oxidation steps were detected on the forward scans for the 4340 (Fig. 5a) and the Aermet100 (Fig. 5c) substrates. For the same solution, one oxidation step was detected when the 300M substrate was tested.

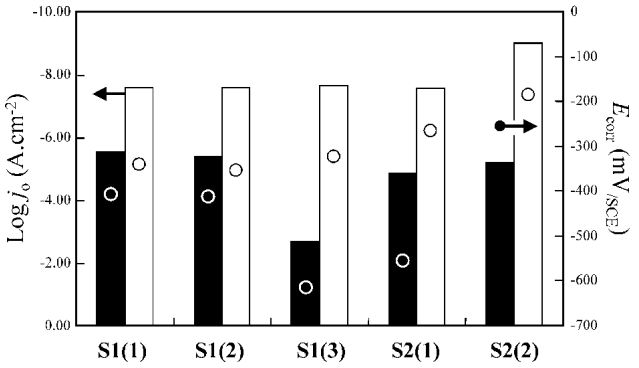

Fig. 6 Corrosion current densities and potentials vs S1 and S2 group of strippers. Black bars and ●, WC-10Co-4Cr coating; and white bars and ○, 4340 substrate

Compared with the S1 group of solutions, the S2 group exhibited no cathodic activity during the reverse scans, therefore indicating that stable oxide or hydroxide thin films covered the substrates. As far as the S2(2) solution was concerned, oxidation steps were detected around 0.35 V for the three substrates (Fig. 5a,c). A rapid glance at the three graphs of Fig. 5 reveals that the three voltammograms for S2(2) are shifted toward more anodic potentials compared with the S2(1) solutions, thus showing the good stabilities of the three substrates in solution S2(2) and confirming the results obtained for j_o and E_{corr} measurements.

3.2 Influence of Stripping Solutions on 4340 Coated Specimens

Corrosion potential and corrosion current density comparisons between 4340 bare plates and coated plates versus the five stripping solutions are shown in Fig. 6. Overall, the stripping solutions were more active on the cermet coating than on the substrate, as can be seen by the higher corrosion current density values exhibited by the coating. The S1(3) and S2(2) solutions were the most active, and dissolution rates were theoretically greater by approximately 100,000 and 6,500 fold, respectively, compared with the dissolution of the bare substrates. This gain of activity is also confirmed by the relative and important potential difference (≈300 mV) between E_{corr} of the bare plate and coated plates. On the other hand, stripping activity was approximately 100, 150, and 500 times greater, respectively, for the S1(1), S1(2), and S2(2) solutions compared with the bare substrates. At this point, it must be stressed that these electrochemical measurements were performed at low and constant hydrodynamic conditions (i.e., air + magnetic agitation) to compare the results. In other words, no attempts were made in the above study to increase the dissolution rate by modifying the mass transfer conditions.

The logarithmic value of the corrosion current for WC-10Co-4Cr in S1(3) was −2.68 A cm^{-2}, which corresponded to a theoretical CPR of 1.22 mpy, assuming that all of the Co and Cr are dissolved and no oxides are formed or oxygen evolution is occurring. From an engineering point of view, this value remains too low even if the efficiency of the S1(3) solution

Table 3 Corrosion Potential Differences Between Bare Plates and Coated Specimens vs the Type of Stripping Solution

	ΔE_{corr}, mV		
Solution	**4340**	**300M**	**Aermet100**
S1(1)	67	14	91
S1(2)	58	6	85
S1(3)	293	221	292
S2(1)	291	266	239
S2(2)	71	13	3

used in an immersion mode could be enhanced using highly turbulent conditions (e.g., ultrasonic agitation), and therefore, industrial stripping conditions should be electrolytic for these kinds of chemical solutions.

The corrosion potential differences among the three bare plates (BP) and the coated specimens (CS) (Eq 2) versus the type of stripping solution are shown in Table 3.

$$\Delta E_{corr} = E_{corr}^{BP} - E_{corr}^{CS} \quad \text{(Eq 2)}$$

Important potential differences (ΔE_{corr} > 220 mV) can be observed for the S1(3) and S2(1) solutions for all steel alloys. In other words, these three substrates could be used safely in such solutions because the coating may be considered to be a sacrificial one. Although all the E_{corr} values for the bare substrates were superior to those of the HVOF coating, the potential differences for the three other solutions were inferior to 15 mV for the 300M alloy immersed in the three stripping solutions and for the Aermet100 immersed in the S2(2) solution. All the other potential differences fell into an intermediate group ($57 < \Delta E_{corr} < 92$ mV).

Polarization curves for the cermet coating dipped in the S1 and S2 stripping solutions are shown in Fig. 7 where two sets of curves can be seen: the 4340 bare substrate and the cermet-coated specimens. As expected, an important anodic activity occurs at low potentials for the cermet coatings. Overall, the difference between the two sets of curves is very well marked: the cermet coating exhibited a very high activity between approximately −0.5 and 0.2 $V_{/SCE}$, while in the same potential range very little activity was observed for the bare substrate: $j < 40$ μA cm^{-2}. These results are very promising regarding criteria (i) and (ii) cited in the Introduction. It also should be noticed that the activity is well marked for the S1(3) stripping solution, where a very high slope characterizes its polarization curve (left-hand side of Fig. 7).

3.3 Coulometric Measurements on 4340 Coated Substrate

To determine the stripping efficiencies of the five solutions, coated 4340 substrates were anodically charged at two different potentials (E_{A1} and E_{A2}; Table 4), and the current was recorded versus time. Using the corresponding cyclic voltammograms, the anodic potentials (E_A) were chosen at two different currents (0.002 and 0.015 A) corresponding to potentials low enough to avoid substrate corrosion.

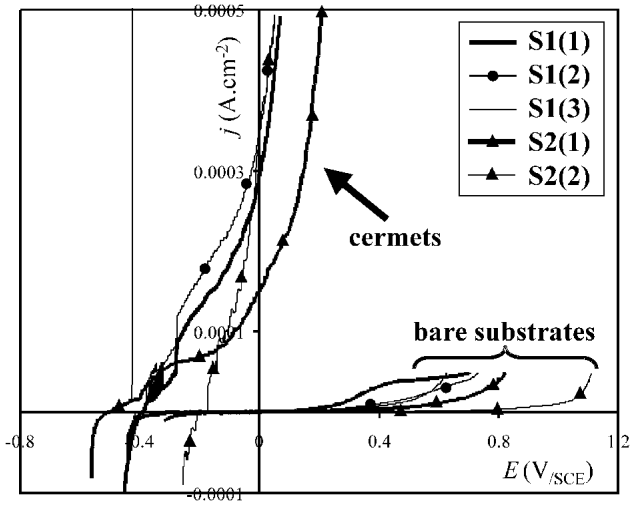

Fig. 7 Cyclic voltammetry plots (forward scans) for the 4340 bare substrate and the WC-10Co-4Cr coatings (v = 5 mV s^{-1} for the S1 and S2 groups)

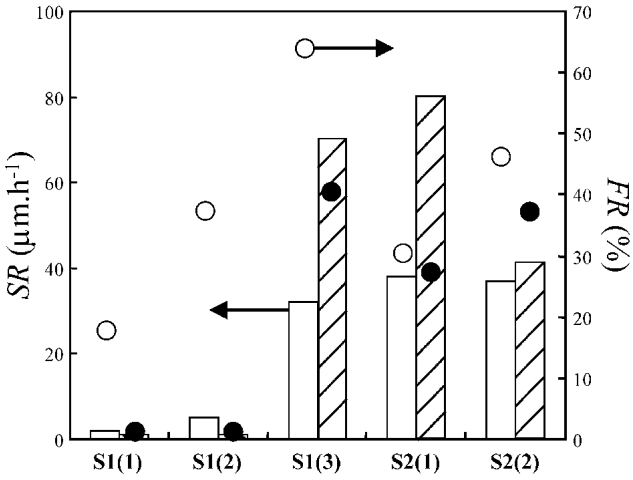

Fig. 8 WC-10Co-4Cr coating SRs and FRs vs the type of stripper. White bars and ○, E_{A1}; and textured bars and ●, E_{A2}

Table 4 Anodic Stripping Potential and Charge for the Five Strippers

Solution	E_{A1}, $V_{/SCE}$	Q_A, C	E_{A2}, $V_{/SCE}$	Q_A, C
S1(1)	+0.36	12	+0.64	92
S1(2)	+0.34	14	+0.59	88
S1(3)	−0.30	54	+0.44	187
S2(1)	+0.57	135	+1.14	317
S2(2)	+0.50	86	+0.84	119

Ten coulometric plots, $i = f(t)$, were performed during 1 h, and the potentials and corresponding charges are shown in Table 4. At high potential, E_{A2}, significant current noise was recorded and was mainly due to the competitive O_2 evolution reaction. Another explanation for this current noise could be

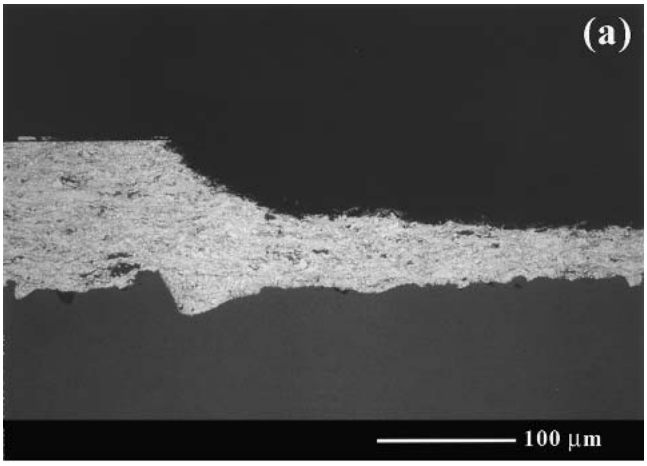

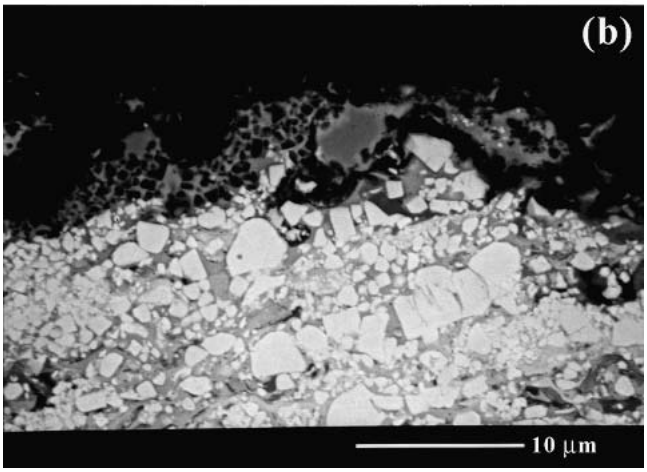

Fig. 9 SEM cross-section micrographs of a WC-10Co-4Cr coating anodically treated (E_{A2} = + 1.14 V) in S2(1) solution. **(a)** magnification ×250; and **(b)** magnification ×3000

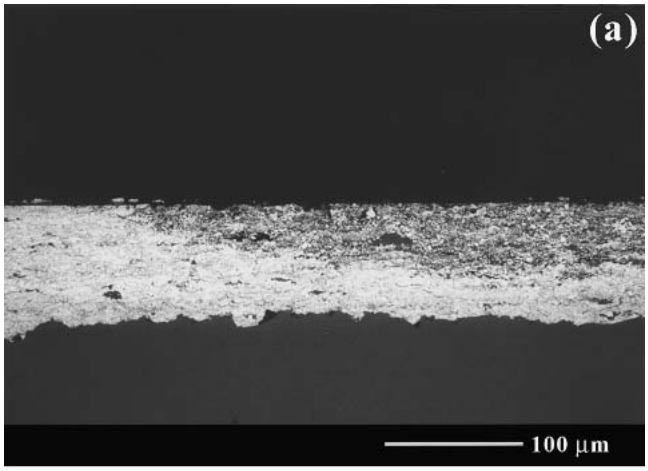

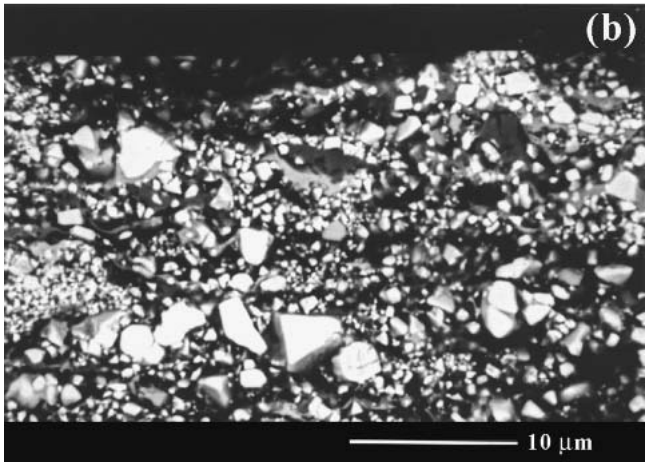

Fig. 10 SEM cross-section micrographs of a WC-10Co-4Cr coating anodically treated (E_{A1} = + 0.57 V) in S2(1) solution. **(a)** magnification ×250; and **(b)** magnification ×3000

due to WC particle removal. The integration of these plots led to the determination of the total applied charge (Q_A). It must be pointed out that the Q_A values were not constant for each of the two E_A values (Table 4). To evaluate the efficiency of the five stripping processes, the SR and the faradic rate (FR) were determined. SR was assessed simply by measuring the stripped thickness of the layer removed after 1 h either at E_{A1} or E_{A2} using cross-section micrographs. To calculate the dissolved mass of Co and Cr, (m_{Co} and m_{Cr} in Eq 3), the densities of these two elements were chosen as 8.9 and 7.19 g cm^{-3}, respectively,[10] and their volume contents inside the WC-10Co-4Cr were chosen at 15.6% and 7.8%, respectively.[10] The theoretical charge, Q_h, to dissolve evenly a cermet layer h ($h = h_i - h_f$) was calculated using Eq 3. Then, using Eq 4, the FR was determined.

$$Q_h = F\left[\left(\frac{m_{Co}}{M_{Co}} n_{Co}\right) + \left(\frac{m_{Cr}}{M_{Cr}} n_{Cr}\right)\right] \quad \text{(Eq 3)}$$

$$FR = \frac{Q_h}{Q_a} \times 100 \quad \text{(Eq 4)}$$

All data are reported in Fig. 8 for the SR and FR values. Comparisons of the SR values among the different solutions used cannot be made since these data were obtained at different Q_A values. In fact, only the FRs show the relative efficiency of the stripping processes in the given constant hydrodynamic conditions established in the experimental procedure. The first main comment is that the S1(1) and S1(2) solutions were almost inactive as far as SR was concerned (Fig. 8). It should be noticed also that at high E_A values the HVOF coating was almost passive regarding these two solutions.

Concerning the three other strippers (S1(3), S2(1), and S2(2)), the processes were overall far more efficient in term of stripping and FR values (Fig. 8) compared with the S1(1) and S1(2) solutions. As far as the FR values were concerned, these were higher at E_{A1} compared with the E_{A2} potential condition. This can be explained by the fact that competitive passivation and/or O_2 evolution reactions are more likely to occur at higher anodic potentials. Meanwhile, the SR values were higher at E_{A2} compared with those found at E_{A1}. At high potential, the O_2 evolution reaction probably created a local agitation that enhanced WC particle removal.

To verify that no galvanic corrosion occurred between the

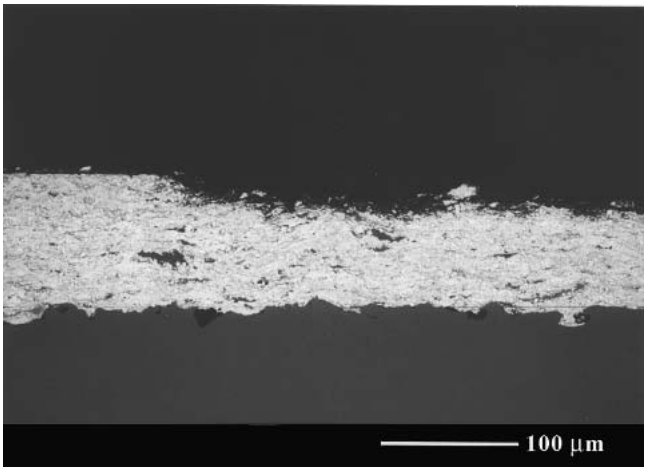

Fig. 11 SEM cross-section micrographs of a WC-10Co-4Cr coating anodically treated (E_{A1} = −0.30 V) in S1(3) solution

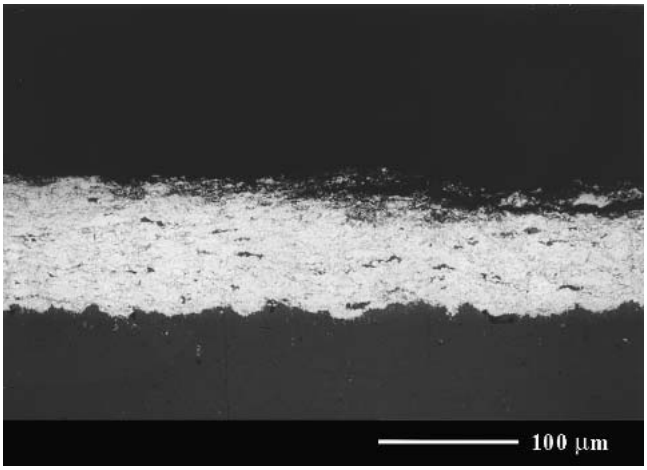

Fig. 12 SEM cross-section micrographs of a WC-10Co-4Cr coating anodically treated (E_{A1} = +0.50 V) in S2(2) solution

Table 5 SR of WC-10Co-4Cr Coatings on 4340 Alloy for Three Different Strippers With Ultrasonic Agitation

	Tubes, U = 4 V		Tubes, U = 6 V		Plates, U = 6 V	
Solution	**SR, μm h^{-1}**	**j, A cm^{-2}**	**SR, μm h^{-1}**	**j, A cm^{-2}**	**SR, μm h^{-1}**	**j, A cm^{-2}**
S1(1)	…	…	…	…	0.29	0.62
S1(2)	0.34	0.09	…	…	0.085	0.97
S1(3)	…	…	83 (a)	0.17	…	…
S1(3)	83	0.09	162	0.17	152	0.78
S2(1)	46	0.07	122	0.17	97	0.78
S2(2)	53	0.07	104 (b)	0.15	61 (b)	0.70

(a) No ultrasonic agitation
(b) U = 7 V

coating and the substrate during the stripping process, coulometric measurements were extended up to 2 h to reach the substrate surface. Coulometric studies showed that a drop in current occurred compared with that seen for 1 h of stripping. This drop was directly associated with the total coating removal. The three different materials (4340, 300M, and Aermet100) stripped by the S1(3), S2(1), and S2(2) solutions were studied by the SEM, and no visible corrosion of the substrate was noticed after the 2 h stripping time.

Therefore, according to selection criteria (i)-(iii) in the Introduction, the best strippers to remove HVOF WC-10Co-4Cr coatings on 4340, 300M, and Aermet100 substrates are S1(3), S2(1), and S2(2). On the other hand, the S1(1) and S1(2) solutions are inactive. The process must be electrolytic but does not need to be very high in potential. According to the FRs, the ranking from the most efficient solution to the least efficient is as follows:

S1(3) > S2(2) > S1(2)

3.4 SEM Observations of the Coatings During Stripping

The SEM study of a WC-10Co-4Cr coating anodically treated with solutions of the S1 group was performed. Only a little material was removed, leaving a thin layer of CoCr matrix having a foam aspect. In fact, O_2 evolution was likely to occur during this stripping process, leading to lower local pH compared with the solution bulk and, thus, decreasing the ability of the material to dissolve since the stripping solutions are effective in very alkaline conditions (Table 2).

SEM observations were also performed on coatings stripped with the other three solutions, and some of the micrographs are displayed in Fig. 9(a,b) (S2(1) solution at E_{A2}), Fig. 10(a,b) (S2(1) solution at E_{A1}), Fig. 11 (S1(3) solution at E_{A1}), and Fig. 12 (S2(2) solution at E_{A1}).

In Fig. 9(a), 10(a), 11, and 12, micrographs were taken near the O-ring location. The portion of the coating on the left-hand part of the image was not stripped, and, close to the other side, material removal was not uniform due to hydrodynamic constraints. However, the stripping uniformity was very good away from the O-ring, particularly at E_{A2} ($E_{A2} > E_{A1}$). At high potential (E_{A2}), the dissolution of the metallic matrix and the removal of the WC particles was concomitant for the S2(1) solution (Fig. 9a), while at low potential (E_{A1}, Fig. 10a) a large amount of loose material remained in the coating and almost all the metallic matrix had dissolved as can be seen at higher magnification (Fig. 10b). This confirmed the hypothesis made previously that at high potential the O_2 evolution reaction probably created a local agitation that enhanced the removal of WC

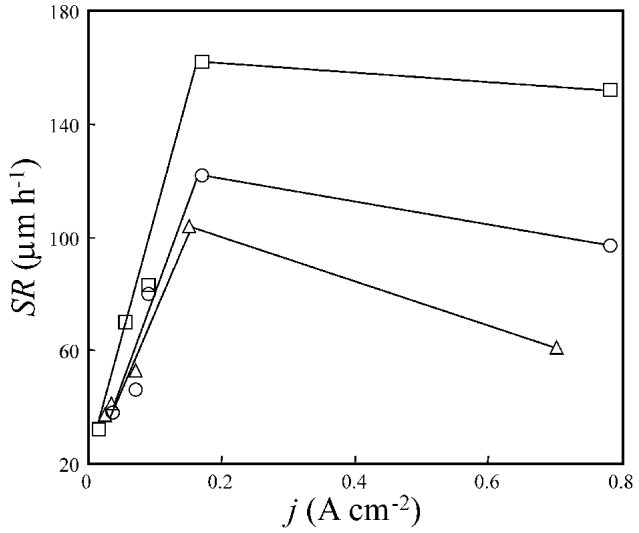

Fig. 13 WC-10Co-4Cr coating (plates and tubes) SRs vs measured current densities. □, S1(3) solution; ○, S2(1) solution; and △, S2(2) solution

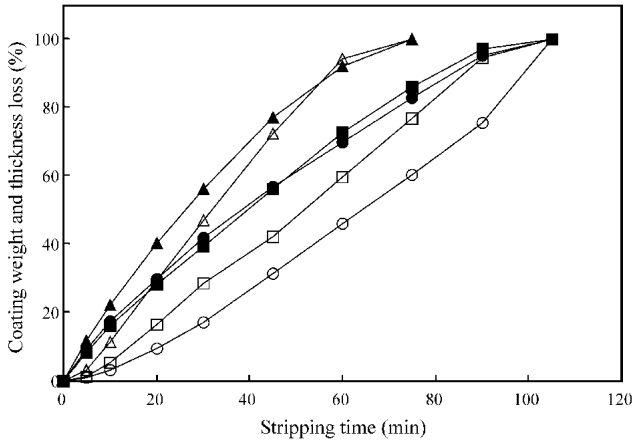

Fig. 14 Thickness and weight percentage losses vs stripping time and type of solutions. S1(3) solution, 6 V: ▲, weight; and △, thickness. S2(1) solution, 6 V: ■, weight; and □, thickness. S2(2) solution, 7 V: ●, weight; and ○, thickness

particles. Thus, the use of a low stripping potential together with high local turbulent conditions (e.g., ultrasonic agitation) leads to high SRs.

When comparing the three different strippers at the low potential E_{A1}, the dissolution was homogenous using the S1(3) solution (Fig. 11) at a relatively low charge (Q = 54 C, Table 4), while the S2(1) solution (Fig. 10a) exhibited very low homogenous dissolution at a high charge (Q = 135 C). The S2(2) solution (Fig. 12) exhibited an intermediate behavior at Q = 86 C.

3.5 Stripping in Industrial Conditions

Cermet stripping on tubes and plates was performed with ultrasonic agitation at three different voltages (U = 4, 6, and 7 V). The industrial operator may adjust U according to Eq 5. It must be pointed out that the potential U corresponds to the overall voltage between the anode and the cathode, and must not be mistaken for the potential E_A of the anode measured with a potentiostat. The SRs were evaluated using linear data fitting, and they are presented in Table 5.

$$U = E_C - E_A - iR_{cell} - iR_{circ} \quad \text{(Eq 5)}$$

The NaOH-based solutions [S1(1) and S1(2)] did not perform well. Stripping was poor, as shown by the very low mean SRs (< 0.34 μm h^{-1}, Table 5) and by the fact that the stripping literally stopped after 1 h, regardless of the applied potential. These results confirmed the potentiodynamic analyses that have shown that in these solutions the cobalt-base matrix passivates.

For the remaining solutions [i.e., S1(3), S2(1) and S2(2)], the SRs can only be compared when current densities are similar, that is, for the tube at 4 V, the tube at 6 or 7 V, or the plate at 6 or 7 V (Table 5). For each of these three cases, and when ultrasonic agitation was used, S1(3) was the most active solution, followed by S2(1) and S2(2). To have a better representation of the influence of the current densities on the SRs (independent of the part geometry), the corresponding graph was plotted and is displayed in Fig. 13, in which the SRs shown in Fig. 8 are also included. Two distinct domains can be defined in Fig. 13, the first one between 0 and 0.2 A cm^{-2}, in which the SRs improved rapidly with current density, and the other one for j > 0.2 A cm^{-2}, in which a slight decrease [more important for the S2(2) solution] was reported for each solution. For the latter case, these decreases are related to mass transfer limitation as well as to the competitive oxygen evolution reactions that occur at high current densities. Independently of the stripping solution, the industrial operator may therefore adjust the stripping potential (U) according to the measured current density by keeping it near 0.2 A cm^{-2}.

To establish the effect of ultrasonic agitation upon stripping efficiency, one test was performed [S1(3) solution and U = 6 V, Table 5] without such agitation. As far as the SR was concerned, a 95% increase (83-162 μm h^{-1}) was reported when the ultrasonic transducers were in use. This result confirmed that, for a given potential, intense local agitation is required to remove loose WC particles and/or metallic matrix chips.

Figure 14 shows the percentage loss of thickness and weight as a function of time for the three active solutions at high U. It was noticed that a shift between the thickness and the weight percentage loss exists where the second one is always higher than the first one. This phenomenon is less pronounced for the S1(3) solution and can be related to SEM observations at E_{A1} = –0.30 V (Fig. 11), since the action of this solution left almost no voids in the stripped part of the coating compared with solutions S2(1) and S2(2) (Fig. 10a and 12). In light of these observations, it is important to notice that stripping took place mainly by the dissolution of the Co-Cr matrix from around the carbides, allowing them to drop out before the final dissolution of the matrix occurred. Thus, the thickness decrease was not directly linked to the weight decrease. Overall, the efficiency of a stripping solution corresponded to its ability to dissolve the Co-Cr matrix uni-

formly from around the WC carbide particles as well as far from them, similar to the behavior exhibited by the S1(3) solution.

4. Conclusions

The use of electrochemical laboratory tests in conjunction with SEM observations on small samples allowed the number of parameters to be narrowed to find solutions for the stripping of WC-10Co-4Cr HVOF coatings before going through the pre-production tests. By using the laboratory test findings, pre-production tests were conducted in near-production conditions, and the parameters to be used on the real parts were established. Correlating the laboratory and the pre-industrial tests, three solutions were found to be efficient for stripping the HVOF WC-10Co-4Cr coatings deposited on high-strength steels: the Meta-nitrobenzane sulfonate solution (60 g/l); NaOH and Na cyanide solution (90 g/l); the Rochelle salt (Na_2CO_3 (184 g/l) + sodium tartarate (75 g/l)) and a commercial nickel stripper. Used in an electrolytic mode, these solutions met the following criteria: they did not etch or strip the three metal substrates (i.e., 4340, 300M, and Aermet100); SRs were high (>80 $\mu m\ h^{-1}$); the coatings were removed uniformly; and no galvanic corrosion between the coating and the steel substrate occurred. Among these three solutions, the cyanide-based solution was the most efficient, with an SR of 162 $\mu m\ h^{-1}$. However, the cyanide-based solution could be harmful or hazardous to the environment if not used properly. Whatever the choice of stripper, it remains very important to proceed with ultrasonic agitation to enhance the overall mass transport and removal of loose WC particles, and to avoid local pH decreases in case of O_2 evolution.

Acknowledgments

The authors wish to thank Michel Thibodeau and Daniel Picard for their precious technical work regarding the SEM studies and the electrochemical assessments of the different stripping solutions.

References

1. H.J. Gibb, P.S.J. Lees, P.F. Pinsky, and B.C. Rooney: "Lung Cancer Among Workers in Chromium Chemical Production," *Am. J. Ind. Med.*, 2000, *38*(2), pp. 115-26.
2. B.D. Sartwell: "HVOF Thermal Spray Coatings Replace Hard Chrome Plating on Aircraft Components," *J. Therm. Spray. Technol.*, 2000, *9*(3), pp. 12-16.
3. B. Dulin and A.R. Nicoll: "Thermal Spray: Advances in Coatings Technology" in *Proc. Nat. Thermal Spray Conf.*, Orlando, FL, Sept. 14-17, 1987, ASM International, Metals Park, OH, 1988, pp. 345-51.
4. M. Dorfman, J. DeFalco, and J. Karthikeyan: "Tungsten Carbide-Coatings for Industrial Applications" in *Proc. 1st Int. Thermal Spray Conf.*, C.C. Berndt, ed., 8-11 May, Montréal, Canada, 2000, pp. 47-78.
5. J.G. Legoux, B. Arsenault, C. Moreau, V. Bouyer, and L. Leblanc: "Evaluation of Four High Velocity Thermal Spray Guns Using WC-10Co-4Cr Cermets" in *Proc. 1st Int. Thermal Spray Conf.*, C.C. Berndt, ed., 8-11 May, Montréal, Canada, 2000, pp. 479-86.
6. K. Legg and B. Sartwell: "Hard Chrome Alternatives Team Update: Improving Performance While Reducing Cost" in Proc. American Electroplaters and Surface Finishers/Environmental Protection Agency (AESF/EPA) Conference for Environmental Excellence, Orlando, FL, Jan 2000.
7. J.D. Nuse, S. Klein, and P. Novotny: "Evaluation of Stripping WC Coatings from Aermet100 Alloy" in *Proc. Hard Chrome Alternative Team (HCAT) Meeting*, Corpus Christi, TX, 15 Dec., 1998.
8. Military standard MIL-STD-871, "Electrochemical Stripping of Inorganic Finishes."
9. E. Jang and R. Kestler: "HVOF Sprayed Coating Stripping Test," AF Contract F04699-98-C-0002 CLIN 1 AY, June 1999.
10. B.R. Marple and J. Voyer: "Improved Wear Performance by the Incorporation of Solid Lubricants During Thermal Spraying" in *Proc. of the 1st Int. Thermal Spray Conf.*, C.C. Berndt, ed., 8-11 May, Montréal, Canada, 2000, pp. 909-18.
11. A.J. Bard and L.R. Faulkner: *Electrochemical Methods, Fundamentals and Applications*, John Wiley & Sons, New York, NY, 1980, p. 106.